

1 **Supplementary Material**

2 **Lowering line tension with high cholesterol content induces a transition from macroscopic**
3 **to nanoscopic phase domains in model biomembranes**

4 Wen-Chyan Tsai and Gerald W. Feigenson*

5 Department of Molecular Biology and Genetics, Cornell University, Ithaca, New York

6 *Corresponding author.

7 *E-mail:* gwf3@cornell.edu (Gerald W. Feigenson)

8

9 *1. Fast cooling technique to acquire desirable size of lipid domains*

10 When GUVs are synthesized with certain lipid compositions, the size of macroscopic Ld + Lo
11 domains may be too large for line tension measurements. Fast cooling is useful for GUV samples
12 in order to break up large macroscopic domains into desirable sizes around 5 μm . Detailed
13 information of applying fast cooling on GUVs in our study is presented in Table S1.

14 Table S1. Fast cooling techniques used in different four-lipid systems

Four lipid systems	Compositions	ρ values	Fast cooling setup	
DSPC/DOPC+POPC/Chol	0.4: 0.4: 0.3	0.15-0.3	Cooled to room temperature over 12 hours, followed by immediate visualization	
		0.4-1.0	Cooled to room temperature over 12 hours, re-heated up to 50 °C and quickly cooled to 0 °C	
BSM/DOPC+POPC/Chol	0.53: 0.2: 0.27 0.5: 0.2: 0.3 0.47: 0.2: 0.33 0.44: 0.2: 0.36 0.42: 0.2: 0.38	0.5-0.7	Cooled to room temperature over 12 hours, followed by immediate visualization	
		0.8-1.0	Cooled to room temperature over 12 hours, re-heated up to 50 °C and quickly cooled to 23 °C	

15 *2. Criteria for line tension measurements*

16 To acquire accurate line tension measurements with minimum deviation, specific criteria are
17 applied for finding appropriate Ld + Lo lipid domains, as described below.

18 1. Circular Ld + Lo lipid domains with sharp phase-contrast boundary are preferred.

19 2. Diameters of Ld + Lo lipid domains should be no larger than 1/5th of the GUV diameters.

20 3. The chosen Ld + Lo lipid domains should be located within the central area of GUV top
21 surfaces. The domains on GUV bottom surfaces must be avoided, due to the interference the
22 GUV surface touching the glass slide.

23 4. One separate lipid domain on the focused central area is preferable. Having two or more
24 adjacent lipid domains in the focused area significantly interferes with natural fluctuations of
25 Ld/Lo boundary.

26 5. A diameter of lipid domains around 5 μm should be used to acquire domain images with clear
27 Ld + Lo phase boundary, especially for certain lipid compositions with higher line tension.

28 6. During line tension measurements using Matlab's Canny edge detection with each 500 frames
29 (the images taken by the microscope), valid frames of each lipid domain must be more than 300
30 in order to be counted as a valid measurement.

31

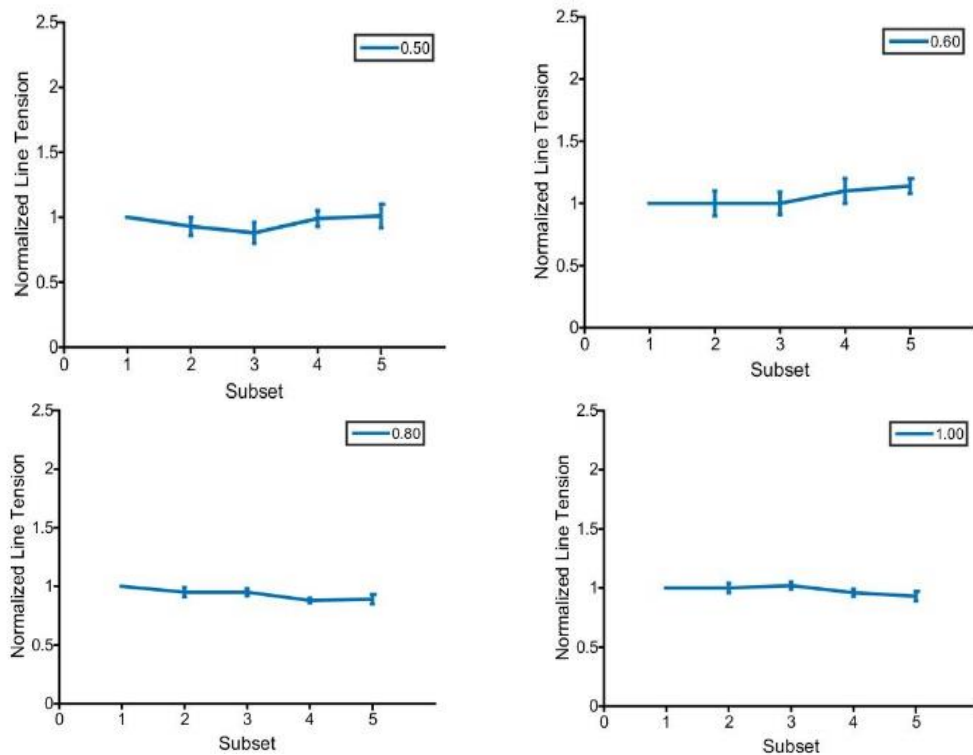
32 *3. Subset analysis*

33 Since the concentration of C12:0 DiI of 0.2 mol % is rather high to achieve sharp boundary
34 contrast between the Ld + Lo phases, light-induced artifacts may occur and cause variation
35 during measurements. Light-induced artifacts can cause breakup, fusion, or an

36 amplitude/frequency change of phase boundary fluctuations. Therefore, it is required to test for
37 any light-induced artifacts by measuring the change in line tension over time. For each lipid

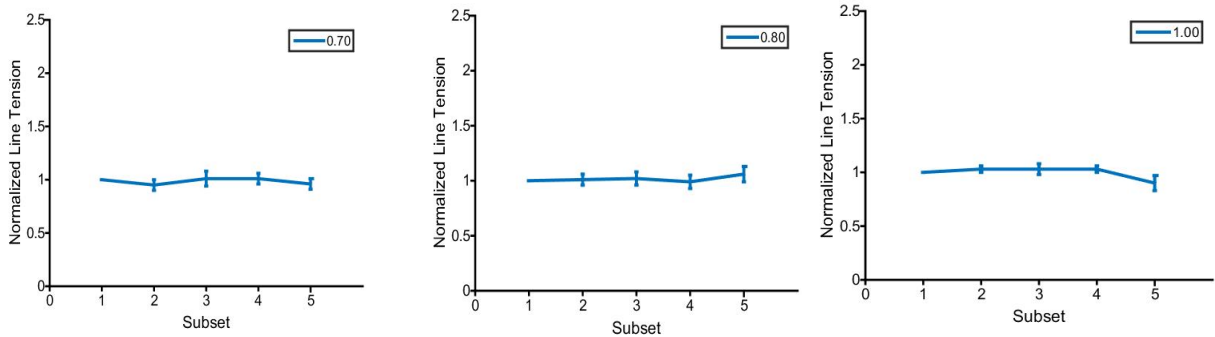
38 domain, the data were split into successive 5 subsets of 100 frames (successive subsets of each
39 time interval for 3 seconds), starting at the first subset from time 0-3 s, the second subset from
40 time 3-6 s, and so forth. For a given domain, the line tension value for each subset was
41 normalized to the line tension value in the first 100 frames. These data were then averaged
42 together over all domains at each ρ value. The subset analyses of line tension measurements for
43 BSM/DOPC/POPC/Chol are presented in Fig. S1. If the variation of normalized line tension is
44 maintained within ± 0.2 , line tension can be accurately determined without light-induced
45 artifacts.

46 BSM/(DOPC+POPC)/Chol=0.53/0.2/0.27



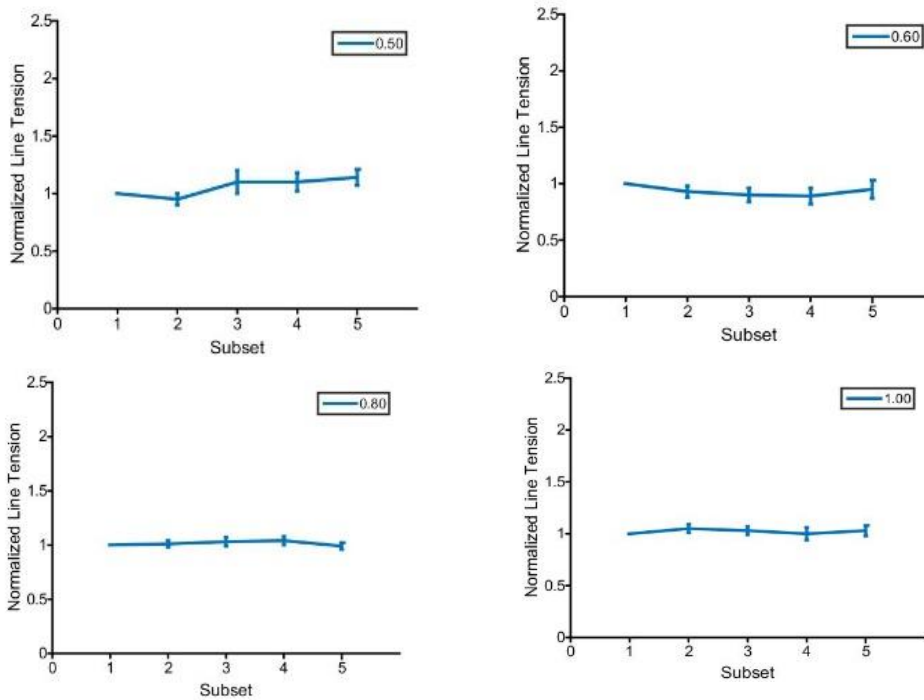
47
48 Fig. S1. Subset analyses for detecting light induced artifacts during line tension measurements.
49 An average line tension of each successive subset of 100 frames is normalized by the line tension
50 in the first 100 frames. The legend indicates the system's ρ value.

51 BSM/(DOPC+POPC)/Chol=0.5/0.2/0.3



52

53 BSM/(DOPC+POPC)/Chol=0.47/0.2/0.33



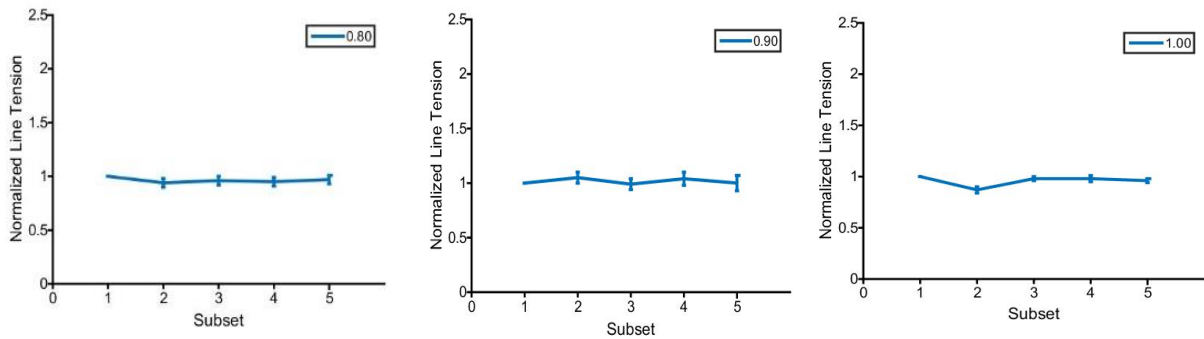
54

55 Fig. S1 (continued). Subset analyses for detecting light induced artifacts during line tension
56 measurements. An average line tension of each successive subset of 100 frames is normalized by
57 the line tension in the first 100 frames. The legend indicates the system's ρ value.

58

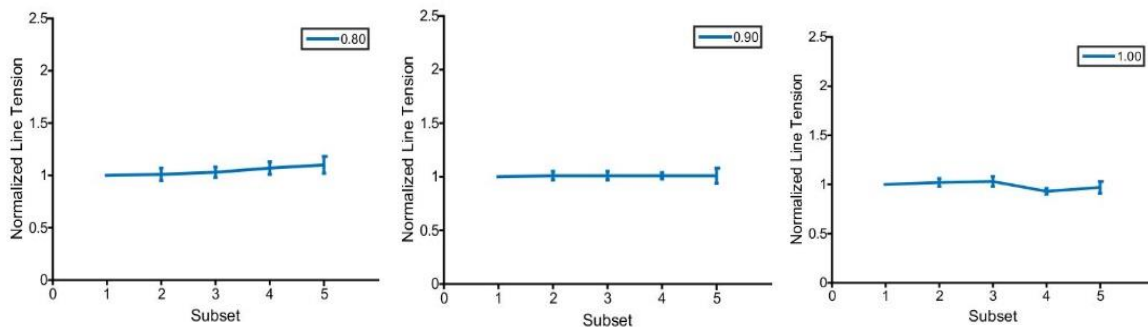
59

60 BSM/(DOPC+POPC)/Chol=0.44/0.2/0.36



61

62 BSM/(DOPC+POPC)/Chol=0.42/0.2/0.38



63

64 Fig. S1 (continued). Subset analyses for detecting light induced artifacts during line tension

65 measurements. An average line tension of each successive subset of 100 frames is normalized by

66 the line tension in the first 100 frames. The legend indicates the system's ρ value.

67

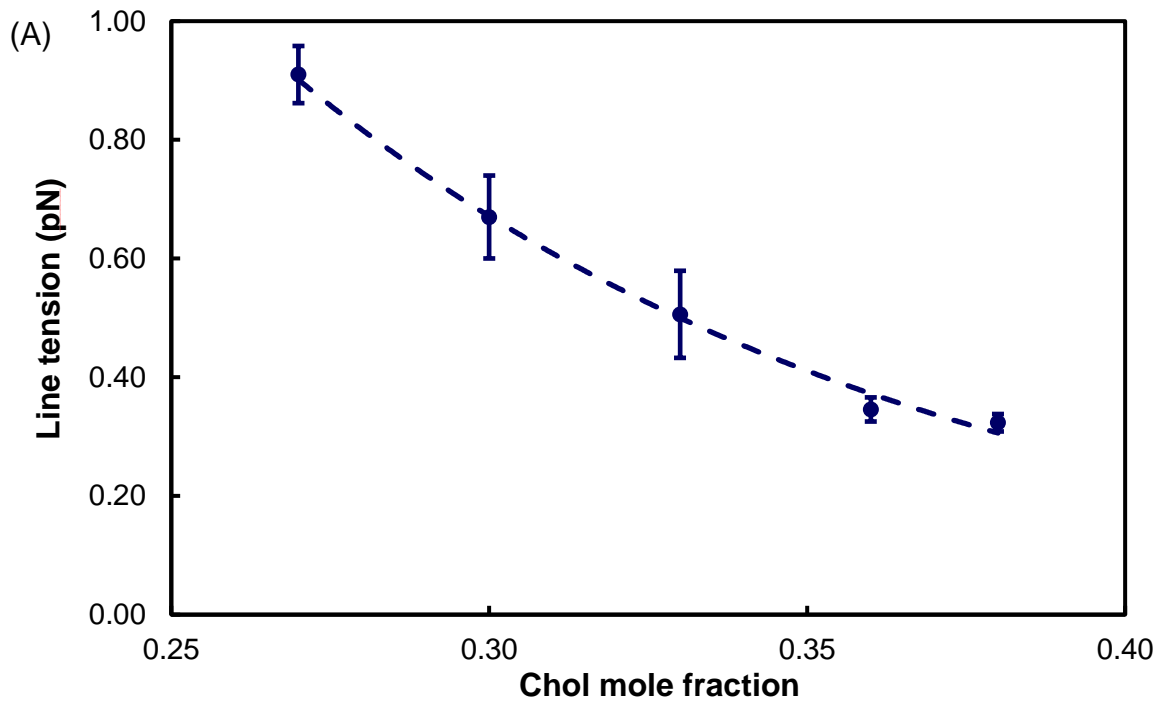
68 4. Correlation of line tension and Chol mole fraction for the BSM/DOPC/Chol lipid mixture

69 In Figure S2 (A), line tension decreases from 0.91 pN to 0.32 pN with overall Chol mole fraction

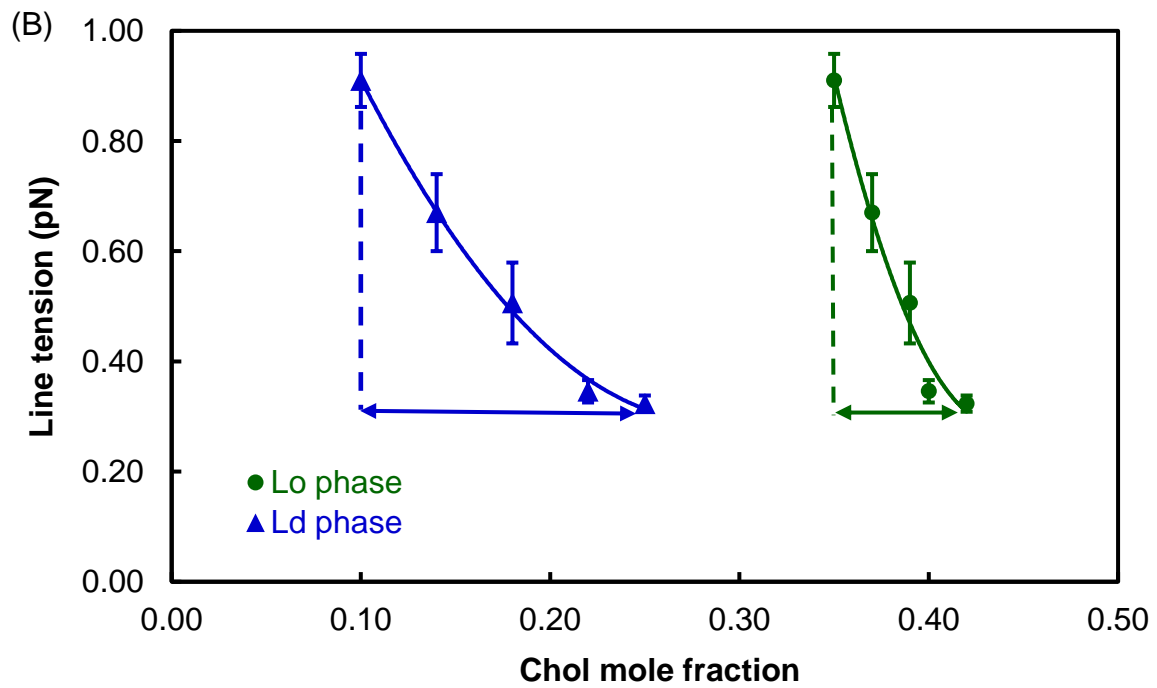
70 ranging from 0.27 to 0.38. Figure S2 (B) shows the decrease of line tension with elevation of

71 Chol content in the Ld or Lo phase, respectively. At $\rho = 1$, Chol mole fraction in the Ld phase

72 increases by 150%, from 0.1 to 0.25, but increases only by about 20% from 0.35 to 0.42 in the
73 Lo phase, as shown by the blue and green arrows, respectively.



74



75

76 Fig. S2. Line tension determined for the BSM/DOPC/Chol lipid mixture ($\rho=1$) with Chol mole
77 fraction increasing from 0.27 to 0.38; (A) Line tension decreases with overall Chol fraction
78 increasing from 0.27 to 0.38; (B) The Chol fraction of Ld increases by 150 %, from 0.1 to 0.25,
79 but increases only by about 20% from 0.35 to 0.42 in Lo, as shown by the blue and green arrows,
80 respectively. Error bars correspond to SE.

81

82 *5. Modulated-phase windows (ρ windows) and line tension of the coexisting Ld + Lo regime*
83 *determined for the BSM/DOPC/POPC/Chol with different Chol mole fractions from 0.27 to 0.38*

84 Modulated-phase windows for the BSM/DOPC/POPC/Chol with different Chol fractions from
85 0.27 to 0.38 are presented in Figure S3. As shown in Figure S4, we found a few GUVs with
86 macroscopic Ld + Lo domains for line tension measurements in lipid mixtures containing Chol
87 fractions of 0.36 and 0.38. During electroformation of GUVs, small osmotic pressure variation in
88 the microenvironment of the swelling chamber may induce a small change in vesicle tension of
89 some GUVs. If this small tension increase occurs for a vesicle that has line tension close to the
90 value needed to form macrodomains, visible Ld + Lo domains could abruptly appear. (detailed
91 explanation presented in Figure S16 of Supplemental Information of our previous study [1]).

92

93

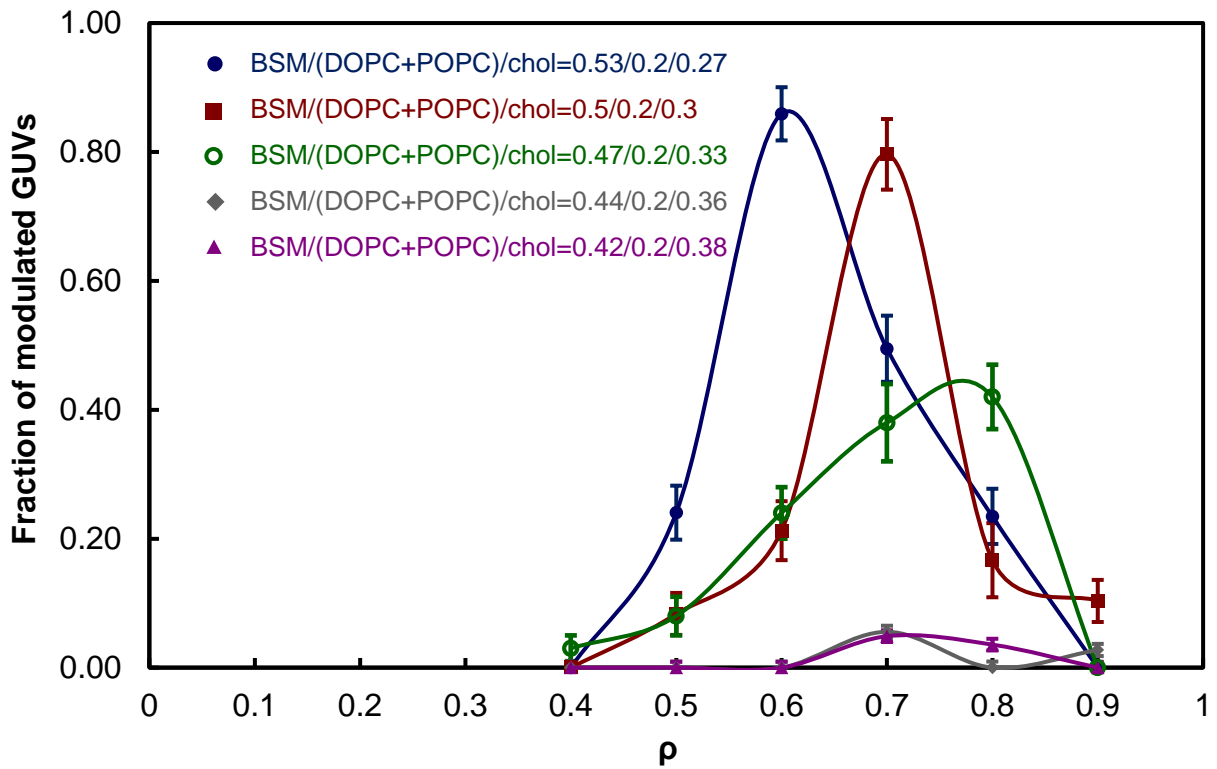
94

95

96

97

98



99

100 Fig. S3. Modulated-phase windows for the coexisting Ld + Lo regime determined for the
 101 BSM/DOPC/POPC/Chol with different Chol mole fractions increasing from 0.27 to 0.38. The
 102 peak of the modulated-phase window shifts to higher ρ values from 0.6 to 0.8, with increasing
 103 Chol mole fraction from 0.27 to 0.33. The fraction of modulated GUVs drastically decreases to
 104 less than 0.1 at higher Chol mole fraction of 0.36 and 0.38. Error bars correspond to SE.

105

106

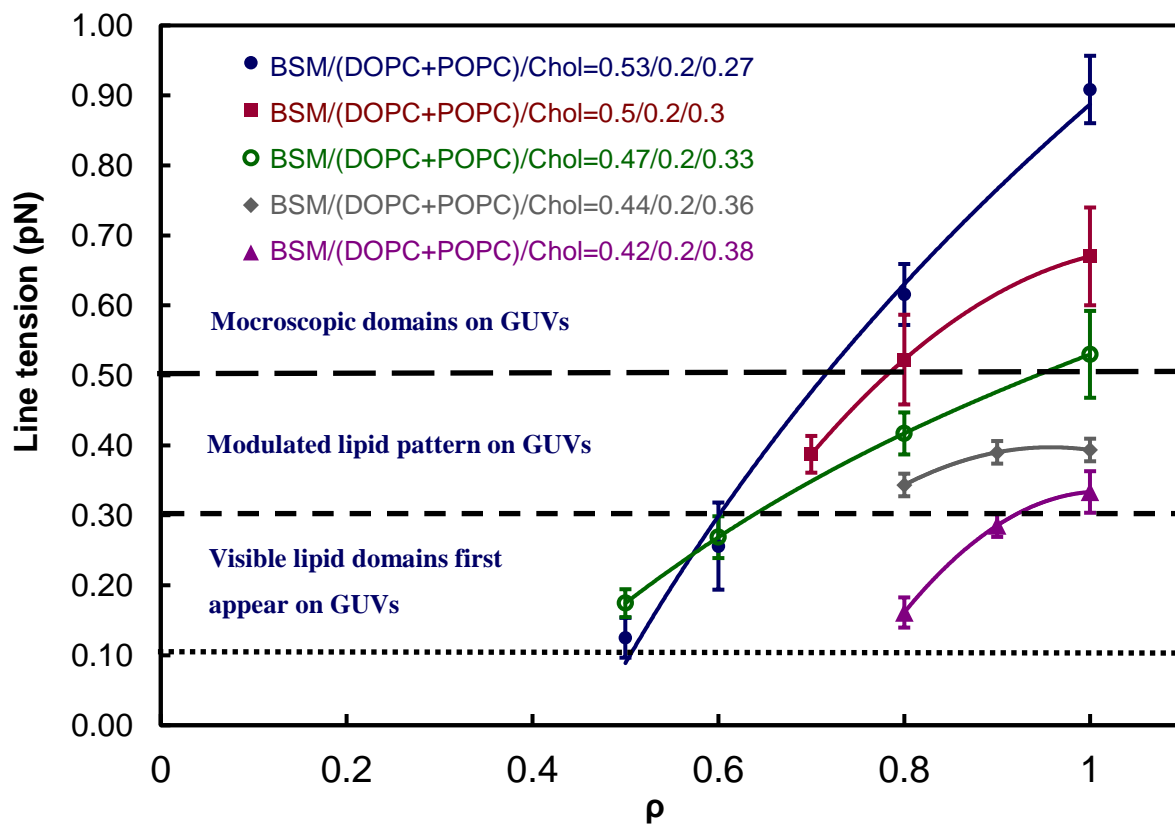
107

108

109

110

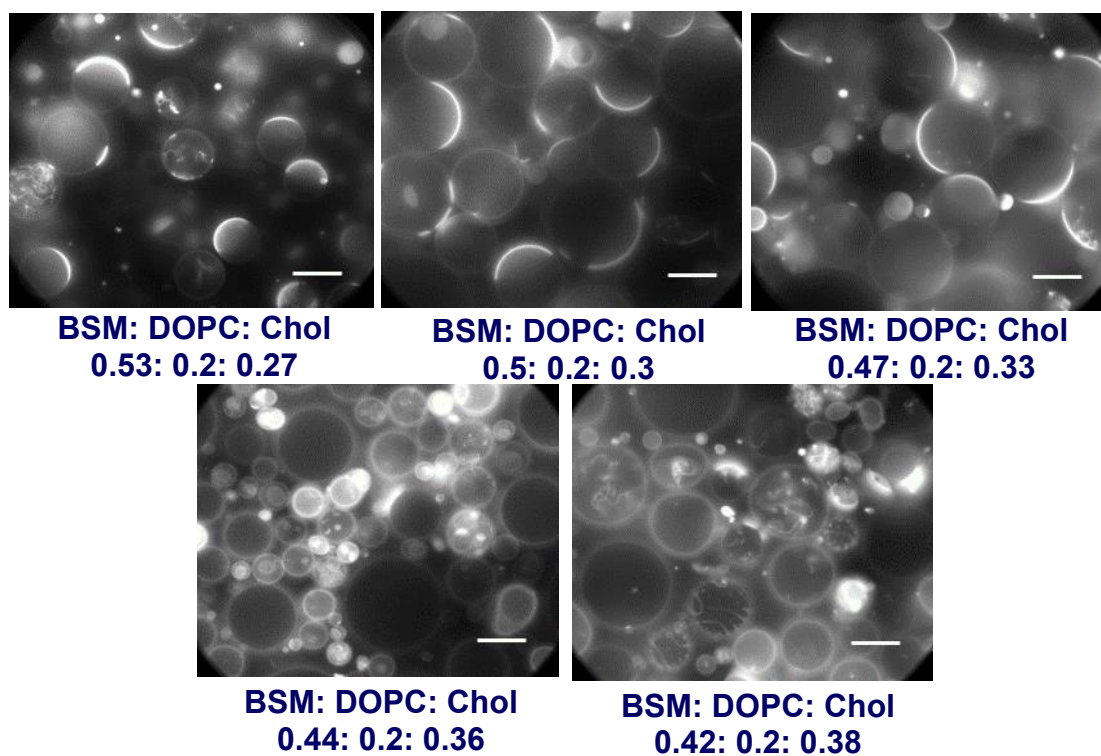
111



112
 113 Fig. S4. Line tension increases as ρ increases for BSM/DOPC/POPC/Chol. In all five mixtures,
 114 visible domains first appear at line tension ranging from 0.1 to 0.3 pN (dotted line). Modulated
 115 GUVs become dominant at line tension between 0.3 to 0.5 pN (dashed line). Above 0.5 pN,
 116 macroscopic GUVs with large and round domains account for the majority (long dashed line).
 117 Compared to those of the lipid mixtures with 0.27 to 0.33 of Chol mole fractions, line tension of
 118 the lipid mixtures with 0.36 and 0.38 of Chol mole fractions at higher ρ values ($\rho = 0.8$ and 1.0)
 119 seem to be relatively lessened. Error bars correspond to SE.

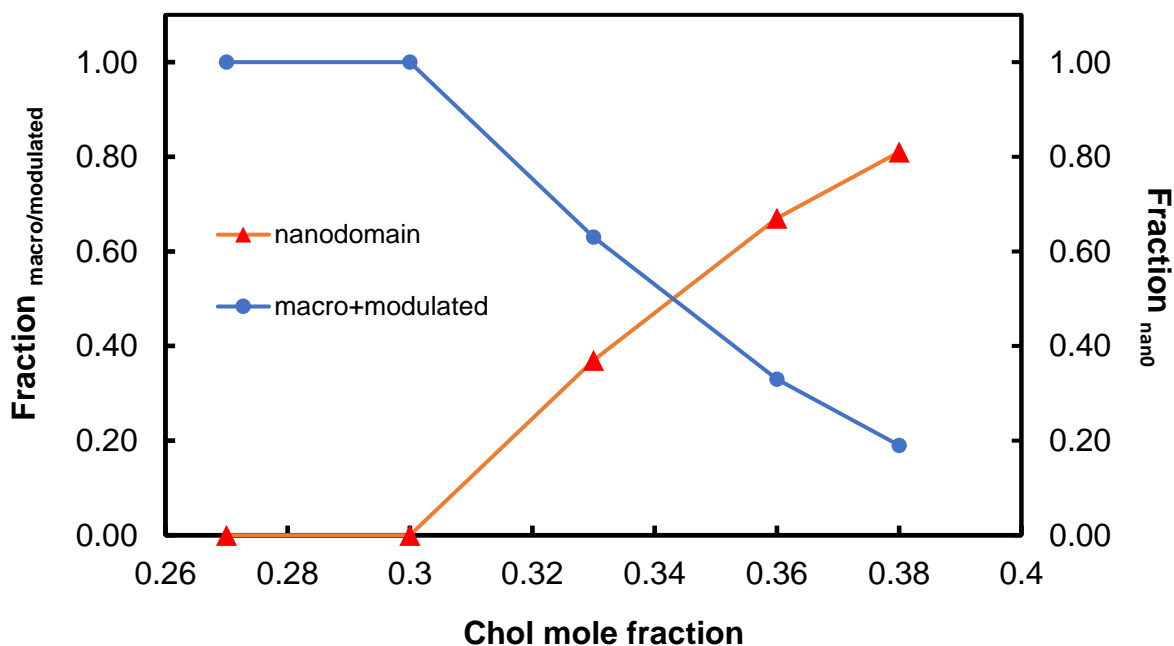
120
 121 *6. Morphology transition of GUVs composed of different BSM/DOPC/Chol lipid mixtures*
 122 Figure S5 shows the phase-morphology images of the GUVs composed of different
 123 BSM/DOPC/Chol lipid mixtures. With Chol mole fraction increased from 0.27 to 0.38,

124 observations suggest that the coexisting Ld + Lo regime turns from macroscopic/modulated
125 domains into nanoscopic domains. As shown in Figure S6, the fraction of visible lipid domains
126 (modulated + macrodomain GUVs) continuously decreased from 1.0 to less than 0.2, while the
127 fraction of uniform GUVs increased with rising Chol content.



128
129 Fig. S5. Morphology of GUVs composed of different BSM/DOPC/Chol lipid mixtures with
130 increasing Chol mole fractions from 0.27 to 0.38. Scale bar: 20 μm .

131
132
133
134
135
136



137

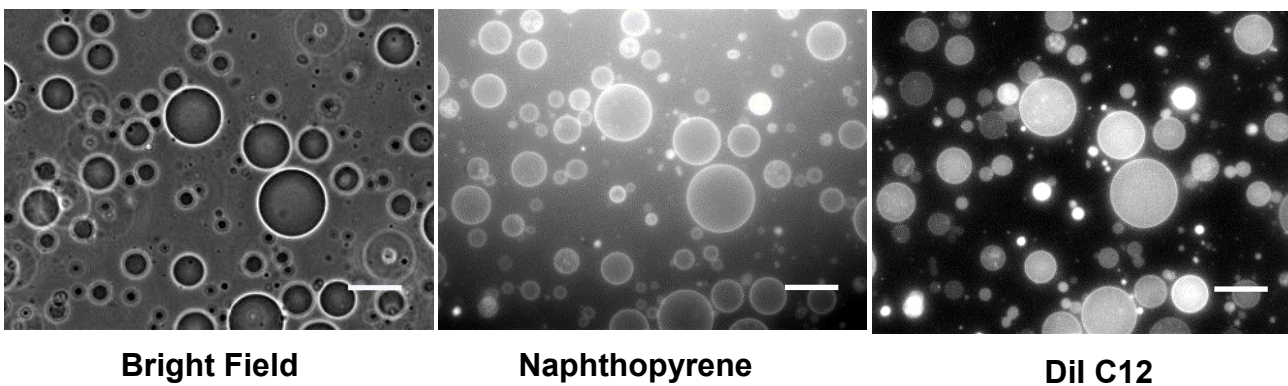
138 Fig. S6. GUV fractions of nanodomains (orange triangle) and visible domains
 139 (macro+modulated; blue circle) in the BSM/DOPC/Chol lipid mixtures with increasing Chol
 140 mole fractions.

141

142 7. Detection of domain fission between *Ld* and *Lo* phases

143 Macrodomains can bud off from the BSM-containing GUV membrane during or after
 144 macroscopic *Ld* + *Lo* phase separation. With DiI C12 favorably diffusing into the *Ld* phase, the
 145 budding may lead to an artifact wherein only homogenous GUVs containing the *Ld* phase *are*
 146 *observed* under fluorescence microscopy, with all *Lo* domain GUVs being dark. To verify
 147 whether the budding effect happened in our study, naphthopyrene was selected for illuminating
 148 the *Lo* phase. To avoid cross-interference of these two fluorescent dyes, excitation wavelengths
 149 for naphthopyrene and DiI C12 were chosen at 405 nm and 561 nm, respectively. Figure S7
 150 shows the images of the GUVs containing BSM/DOPC/Chol under bright field and excited

151 fluorescence of 405 nm and 561 nm. All of the images exhibit the same distribution of GUVs.
152 No budding artifact occurred among the GUVs, that would have made pure Lo GUVs invisible.



153
154 Fig. S7. Detection of the budding effect among the BSM-containing GUVs:
155 BSM:DOPC:Chol=0.42: 0.2: 0.38. Naphthopyrene: Lo-favoring dye with excited fluorescence at
156 405 nm; DiI C12: Ld-favoring dye with excited fluorescence at 561 nm. Scale bar: 20 μ m.
157